Oikos

OIK-01539
Fort, H. 2014. Quantitative predictions of pollinators' abundances from qualitative data on their interactions with plants and evidences of emergent neutrality. – Oikos doi: 10.1111/oik.01539

Appendix 1
Data set

The data set of plant-pollinator interactions comprises a total of 38 mutualistic networks (Rezende 2007, NCEAS 2014), spanning a broad geographic range from arctic to tropical and temperate and Mediterranean. The list of networks, including their richness S_A and corresponding locations is:

Number	ode name	S_A	Quantitative matrix	Locality
1	ARR1	101	NO	Cordón del Cepo, Chile
2	ARR2	64	NO	Cordón del Cepo, Chile
3	ARR3	25	NO	Cordón del Cepo, Chile
4	BAHE	102	YES	Central New Brunswick, Canada
5	BEZE	13	YES	Pernambuco State, Brazil
6	CLLO	275	NO	Pikes Peak, Colorado, USA
7	DIHI	61	YES	Hickling, Norfolk, UK
8	DISH	36	YES	Shelfanger, Norfolk, UK
9	DUPO	38	NO	Tenerife, Canary Islands
10	EOL	118	NO	Latnjajaure, Abisko, Sweden
11	EOLZ	76	NO	Zackenberg
12	ESKI	13	NO	Mauritius Island
13	HERR	179	NO	Doñana Nat. Park, Spain
14	HOCK	81	NO	Hazen Camp, Ellesmere Island, Canada
15	INPK	85	YES	Snowy Mountains, Australia
16	KEVN	27	NO	Hazen Camp, Ellesmere Island, Canada
17	KT90	679	YES	Ashu, Kyoto, Japan
18	MED1	45	NO	Laguna Diamante, Mendoza, Argentina
19	MED2	72	NO	Rio Blanco, Mendoza, Argentina
20	MEMM	79	YES	Bristol, England
21	MOMA	18	YES	Melville Island, Canada
22	MOTT	44	YES	North Carolina, USA
23	MULL	54	NO	Galapagos
24	OFLO	28	NO	Flores, Açores
25	OFST	42	NO	Hestehaven, Denmark
26	OLAU	55	NO	Garajonay, Gomera, Spain
27	OLLE	56	YES	KwaZulu-Natal region, South Africa
28	PERC	36	NO	Jamaica
29	PRAP	60	NO	Arthur's Pass, New Zealand
30	PRCA	139	NO	Cass, New Zealand

31	PRCG	118	NO	Craigieburn, New Zealand
32	PTND	666	NO	Daphní, Athens, Greece
33	RABR	53	NO	Guarico State, Venezuela
34	RMRZ	49	NO	Canaima Nat. Park, Venezuela
35	SCHM	33	YES	Brownfield, Illinois, USA
36	SMAL	34	YES	Ottawa, Canada
37	SMRA	130	NO	Chiloe, Chile
38	VASI	30	YES	Llao Llao, Argentina

For 13 of these networks (marked in gray) there were quantitative interaction matrices from which empiric species relative abundances $\{n_a\}$ for pollinators were inferred: BAHE, BEZE, DIHI, DISH, INPK, KT90, MEMM, MOMA, MOTT, OLLE, SCHM, SMAL and VASI.

Correlation relative abundance − degree.

The Pearson correlation between n_a and D_a is strong i.e. > 0.6 in most cases and in all the cases is significant (Fig. S1).

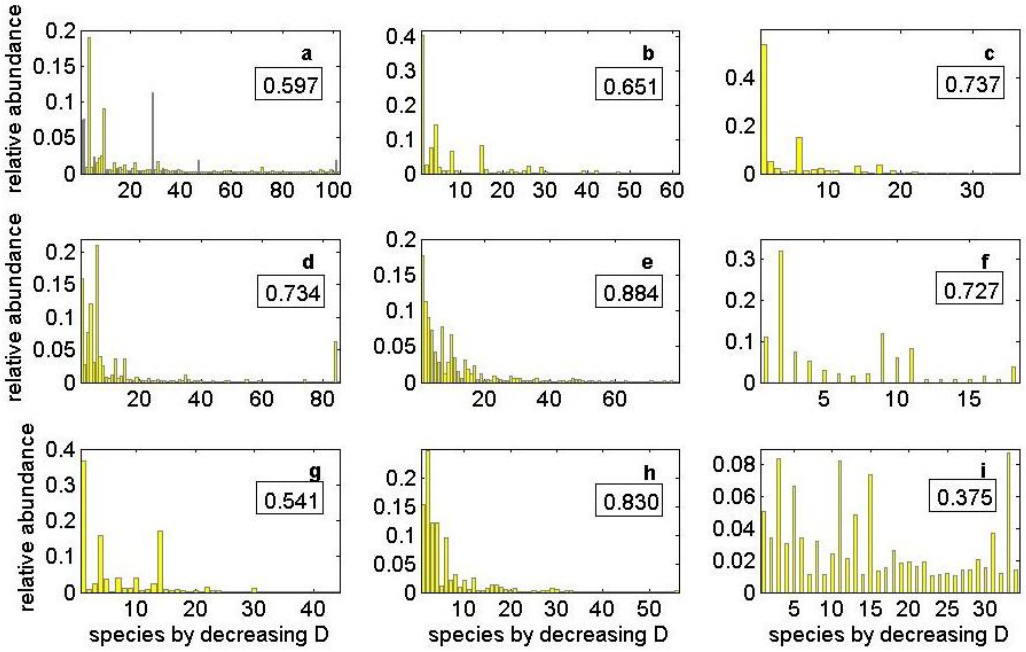

Figure S1 Empiric RAPS for nine plant-pollinator networks for which there are quantitative interaction matrices: BAHE (a), DIHI (b), DISH (c), INPK (d), MEMM (e), MOMA (f), MOTT (g), OLLE (h) & SMAL (i). Insect species are numbered according to decreasing degree D_a. The numbers in boxes correspond to the correlation between n_a and D_a, which is strong i.e. > 0.6 in most cases and in all the cases is significant (pValue < 0.01 for A-H and pValue < 0.05 for I).

More refined calculations of the competition coefficients and the RAPS they predict.

From the $\{n_a\}$ it is possible to obtain a less coarser estimation of the resource utilization distribution f_a for each pollinator species and then to compute more refined competition coefficients, that improved the matching between the theoretical and empirical RAPS. The interaction frequency of animal species a with plant species p is thus obtained as

$$f_{ap} = q_{ap} / \sum_{p=1}^{S_P} q_{ap}. \qquad (S1)$$

The f_{ap} are the components of the resource utilization distribution f_a for each animal species. Each $\alpha_{aa'}$ was computed from (6) as the normalized scalar product or overlap $O_{aa'}$ of the resource utilization distributions of these two species:

$$\alpha_{aa'}^{\text{quant}} = N_{aa'} O_{aa'} = \frac{N_{aa'} \sum_{p=1}^{S_P} f_{ap} f_{a'p}}{\sum_{p=1}^{S_P} f_{ap} f_{ap}}. \qquad (S2)$$

In Fig. S2 we show a comparison between theoretical RAPS using qualitative vs. quantitative information for the plant-pollinator interactions.

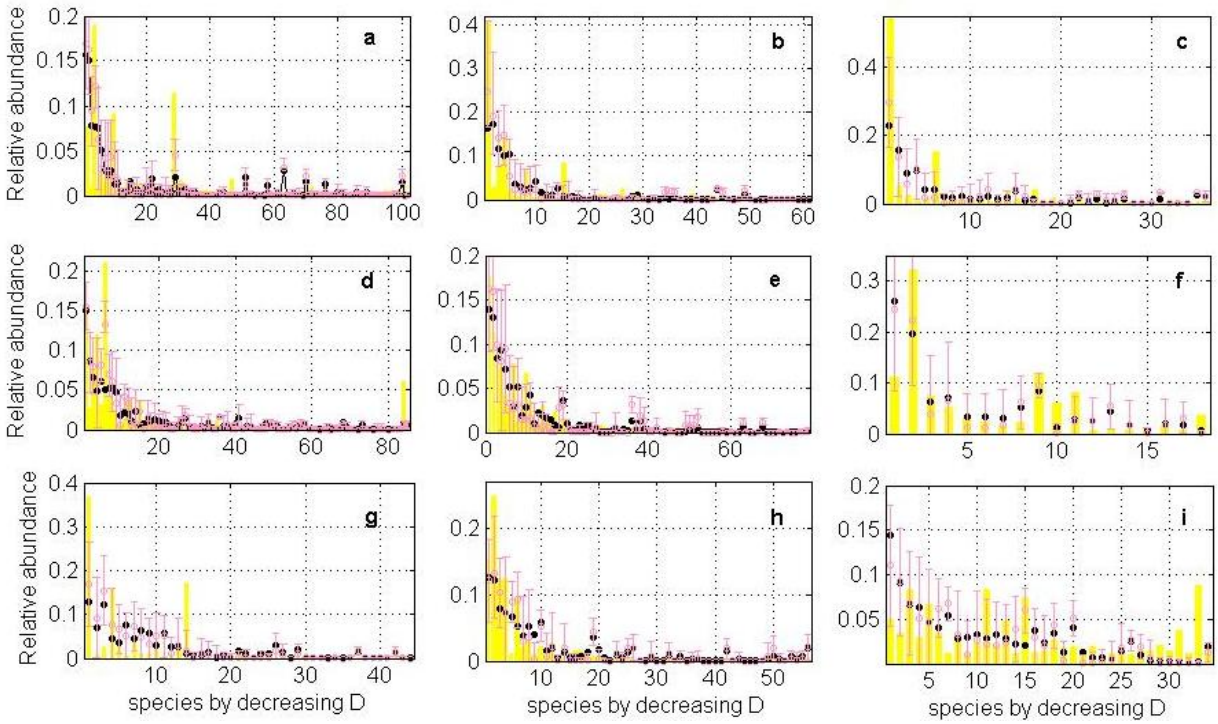

Figure S2 Comparison between theoretical RAPS produced by competition matrices computed from qualitative and quantitative interaction matrices. Relative abundances of pollinator species: empiric RAPS (yellow bars); theoretical RAPS obtained for $\boldsymbol{\alpha}$ computed from adjacency matrices g_{ap} (black) and for $\boldsymbol{\alpha}$ computed from quantitative interaction matrices q_{ap} (pink with errors = 1 std for 200 simulations). Results for the nine plant-insect networks for which there are quantitative interaction matrices available: BAHE (a), DIHI (b), DISH (c), INPK (d), MEMM (e), MOMA (f), MOTT (g), OLLE (h) & SMAL (i). Insect species are numbered according to decreasing degree D_a.

Block structure of competition matrices along a niche axis.

Suppose N species randomly distributed along a niche axis and each species i represented by a normal distribution $P_i(x) = \exp[-(x - \mu_i)^2/(2\sigma_i^2)]$ centred at μ_i and with a standard deviation σ_i, which measures the width of its niche. Therefore the competition coefficients α_{ij} can be computed by the MacArthur-Levins niche overlap (MLNO) formula (MacArthur & Levins 1967):

$$\alpha_{ij} = \frac{\int_{-\infty}^{\infty} P_i(x)P_j(x)dx}{\int_{-\infty}^{\infty} P_i^2(x)dx} = e^{-\frac{(|\mu_i-\mu_j|)^2}{4\sigma^2}}, \qquad (S3)$$

and this matrix looks like Fig. S3.

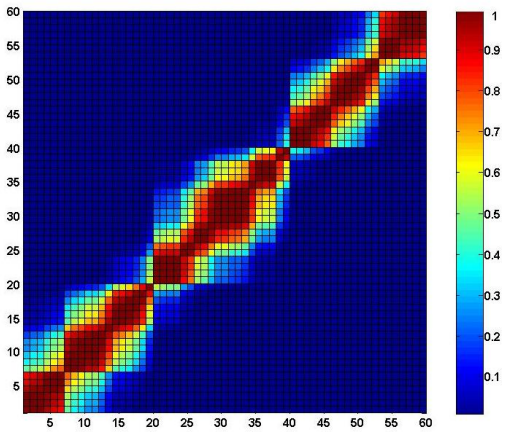

Figure S3 Block structure for a competition matrix of species randomly distributed along a niche axis *x*. The competition matrix α_{ij} generated by eq. (*S3*), its diagonal corresponds to x ($0 \leq x \leq 1$), results for $N = 60$ species all with the same niche width $\sigma = 0.05$. Colour code: blue (dark red) corresponds to $\alpha_{aa'} = 0$ (1).

To build the corresponding niche axis for each community of pollinators we considered permutations of rows and columns of α in order to group together all the species that strongly compete by resources (plants). One way to do that is by using a simulating annealing method in which distances from diagonal are penalized (Methods).When we performed this grouping according niche proximity then a block structure, like the one shown in Fig. S3, emerged. For instance when the pollinators of the PRAP (Rezende 2007) network are sorted in decreasing order according to their degree D (i.e. from $D = 9$ to 1) the competition matrix looks like Fig. S4a. When species were ordered along x, we got Fig. S4b.

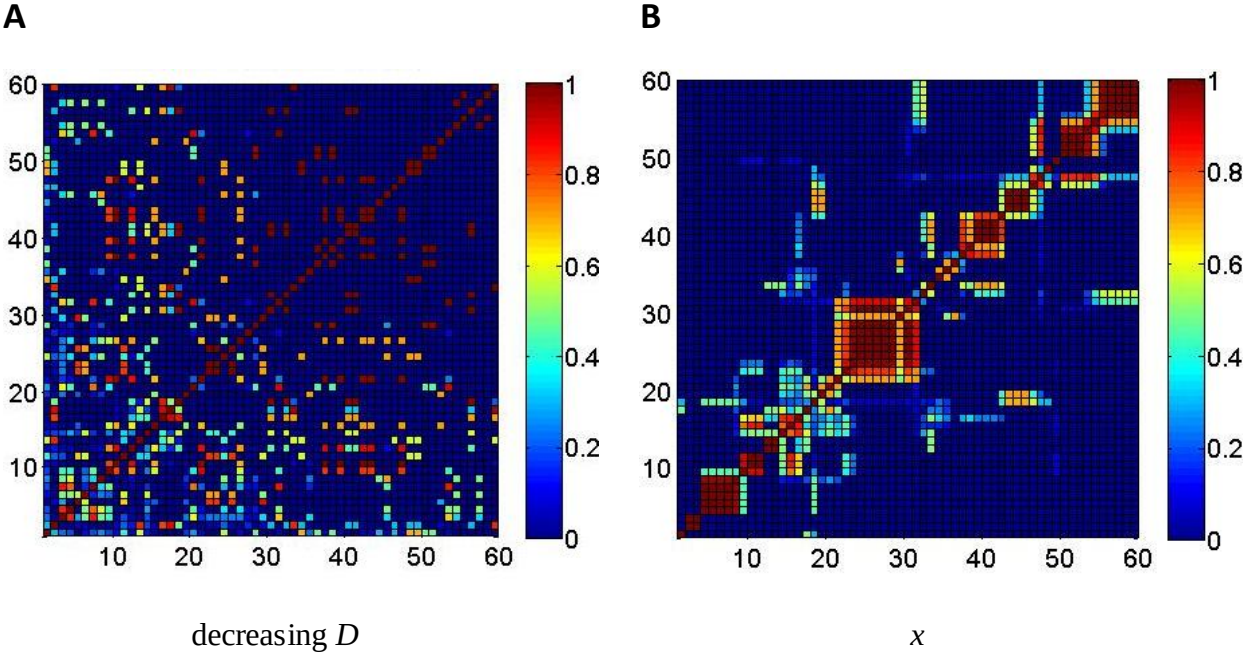

Figure S4 Competition (Jaccard) matrices between pollinators for D-order vs. niche order. PRAP network, of $S_A = 60$ pollinator species. Red sites correspond to high competition ($J_{aa'}$ close to 1) while blue sites correspond to low competition ($J_{aa'}$ close to 0). By definition $\alpha_{aa} = J_{aa} = 1$, corresponding to unit squares at the diagonal. (a) Species ordered by decreasing degree *D*. (b) Species ordered by their niche (integer) 'position' x_a. This competition matrix was obtained after a simulating annealing procedure to reorder rows and columns of the matrix shown in (a).

Multimodal SAD

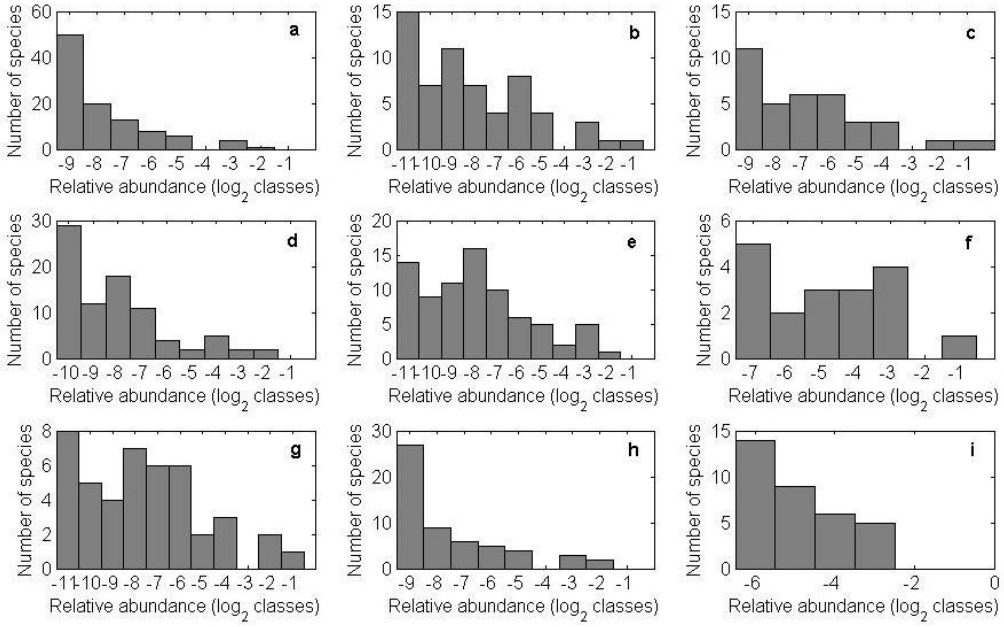

Figure S5 Preston like diagrams for observed SAD. DIHI (b), DISH (c), INPK (d), MEMM (e), MOMA (f), and MOTT (g) look multimodal to the naked eye. Indeed the DIP test (Hartigan 1985) measure that all the histograms except the one for the SMAL (i), are multimodal (p-Value < 0.05).

Robustness of theoretical predictions: nonlinear Lotka-Volterra competition equations.

To test the robustness of the theoretical predictions under changes of the linear Lotka-Volterra competition equations (1) by non-linear ones, we simulated quadratic dependencies in the parenthesis of eq. (1) i.e.

$$\frac{dN_a}{dt} = r_a N_a \left(1 - \sum_{a'=1}^{S_A} \alpha_{aa'} \left(\frac{N_{a'}}{K_a}\right)^2\right), \qquad a = 1, \ldots, S_A \,. \qquad (S4)$$

The results didn't change dramatically as it is shown in Fig. S6 for MEMM.

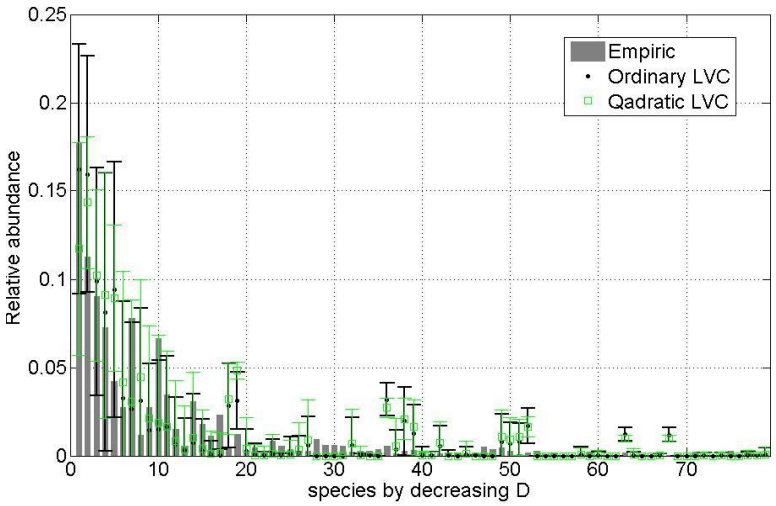

Figure S6 Non-linear versus linear LVC model. No important differences were observed.

Performance of biodiversity indices

Let us define the differences between theoretical and empirical biodiversity indices by $\delta H = H_{theo} - H_{emp}$ and $\delta SG = SG_{theo} - SG_{emp}$. A general pattern, for all the analyzed nine networks, is that $\delta SG < \delta H$. This is shown for the INPK mutualistic network in Fig. S7. The explanation of why SG works better than H is that the process of averaging over simulations introduces fluctuations that are relatively larger (higher coefficient of variation) in the populations of rare species. And H is known to be more sensitive to variations in rare species than SG.

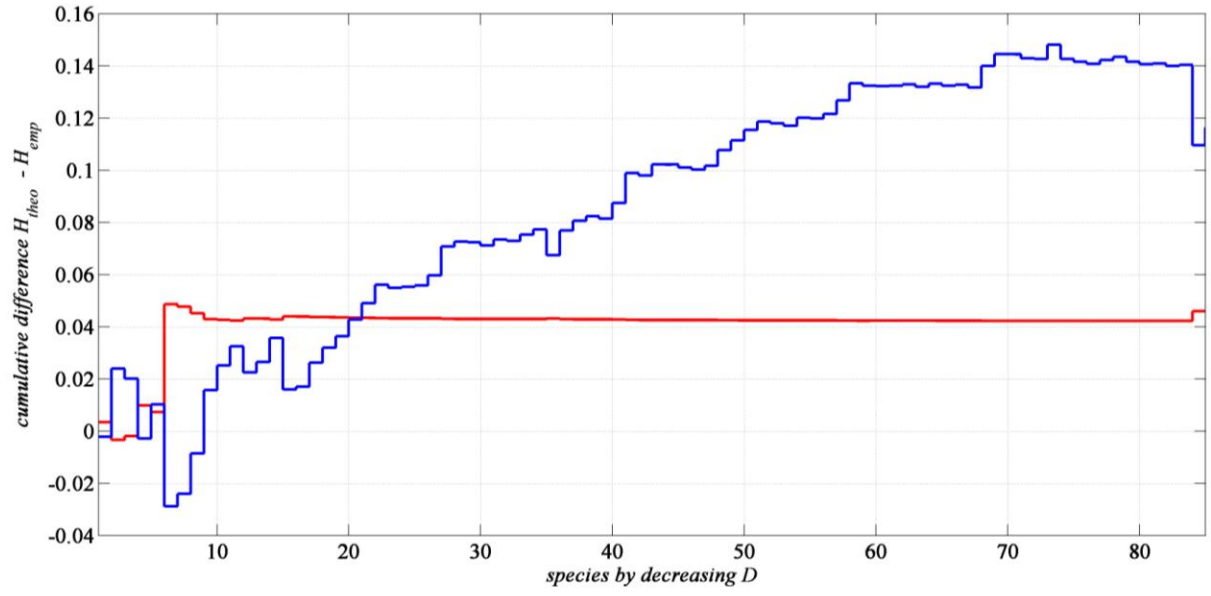

Figure S7 Analyzing the difference between theoretical and empirical biodiversity indices for INPK network (S_A= 85). Cumulative contributions to $\delta H = H_{theo} - H_{emp}$ (blue) and to $\delta SG = SG_{theo} - SG_{emp}$ (red) are shown. For example, the first point corresponds to $\delta H_1 = -(n_1^{theo} \ln n_1^{theo} - n_1^{emp} \ln n_1^{emp})/\ln 85$, the second point corresponds to $\delta H_2 = \delta H_1 - (n_2^{theo} \ln n_2^{theo} - n_2^{emp} \ln n_2^{emp})/\ln 85$, and so on. On the one hand we can see that δSG quickly stabilizes close to its value of approximately 0.05 when taking into account the most abundant species. On the other hand rare species have important contributions to $\delta H \cong 0.11$.

Agreement between predicted and empirical RAPS for four additional networks (not shown in the article)

Figure S8 shows theoretical and empirical relative abundances of pollinator species (RAPS) for these four networks: BEZE, KT90, SCHM and VASI (NCEAS 2014). , the agreement between predicted and empirical RAPS varies from network to network. In particular it is impressively good for BEZE in panel a ($d_{\text{emp-theo}} = 0.98$).

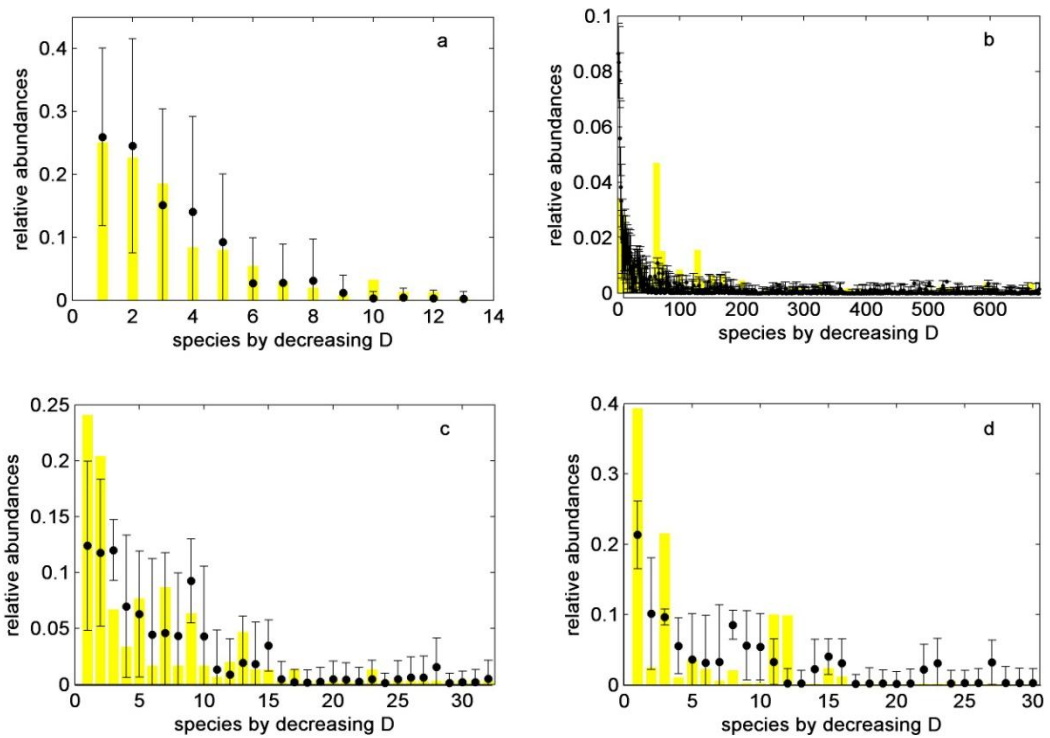

Figure S8 Predicted and observed RAPS. Empiric (yellow bars) and theoretical (black with errors = 1 std for 100 simulations) RAPS for plant-pollinator networks: BEZE (a), KT90 (b), SCHM (c) & VASI (d) (NCEAS 2014). Insect species are numbered according to decreasing degree D_a.

References

Hartigan, J. A. and Hartigan, P. M. 1985. The dip test of unimodality. - Ann. Stat. 13: 70-84.

Jaccard, P. 1901. Étude comparative de la distribution florale dans une portion des Alpes et des Jura. – Bull. Soc. Vaudoise Sci. Nat. 37: 547–579.

MacArthur, R. H. and Levins, R. 1967. The limiting similarity, convergence and divergence of coexisting species. - Am. Nat. 101: 377–385.

NCEAS 2014. <www.nceas.ucsb.edu/interactionweb/resources.html>

Rezende, E. et al. 2007. Non-random coextinctions in phylogenetically structured mutualistic networks. - Nature 448: 925-928.